Fixed-phase diffusion Monte Carlo study of activation gap and skyrmion excitations of a $\nu = 1$ system in the presence of charged impurities

Tongzhou Zhao
Department of Physics, 104 Davey Lab, Pennsylvania State University, University Park, Pennsylvania 16802, USA

(Received 16 June 2021; revised 26 August 2021; accepted 27 August 2021; published 9 September 2021)

The discrepancy between the theoretically calculated and experimentally measured activation gaps in quantum Hall effect has long been a puzzle. We revisit this issue in the context of the $\nu = 1$ quantum Hall state, while also incorporating the skyrmion physics. We find that the finite width and the Landau level mixing effects are not sufficient to explain the observed activation gap. We further show that the presence of charged impurities located adjacent to the quantum well can cause a significant reduction in the activation gap, while also causing a suppression of the skyrmion size.

DOI: 10.1103/PhysRevB.104.115303

I. INTRODUCTION

Ever since the discovery of the fractional quantum Hall effect (FQHE) [1,2], many theoretical achievements have been made [3,4] and a lot of experiment discoveries are successfully explained. However, a lot of questions remain. One of them is to quantitatively understand the excitation gap of FQHE states. The experimentally measured gaps [5–11] are found to be significantly lower than the theoretically predicted ones [12–17]. We note here that even for the filling factor $\nu = 1$, the theoretical value of the gap to charged excitations [18–21] is much greater than the values observed in experiments [22,23]. That is the discrepancy we address in this work, with the belief that an understanding of it will help resolve the discrepancy for the fractional quantum Hall gaps.

In the noninteracting picture, the ground state is fully polarized and the low-energy excitation of the system in the small Zeeman energy limit consists of a quasiparticle and a quasihole pair, where a single spin-up electron is flipped and added to the lowest Landau level of the opposite spins. The energy of this excitation is modified substantially due to interaction, thus producing a gap that is much larger than the Zeeman splitting. There is another effect that lowers the gap, which has to do with the formation of the so-called skyrmion excitations. This appears most dramatically at zero Zeeman energy. Here, the ground state is still fully spin polarized due to exchange effects. However, exact diagonalization studies by Rezayi [24,25] showed that even the removal of a single electron from the ground state (or adding one more electron into the system) makes the system a spin singlet. This spin-singlet state was later identified by Sondhi *et al.* [26] to be the skyrmion state. This has lower energy than the state involving the flip of the spin of a single electron. For finite Zeeman energies, a skyrmion of a finite size is obtained [18,19,25–28].

The activation gaps predicted by the skyrmion physics [18,19] are significantly larger than experimental values measured in GaAs quantum wells [22,23]. Therefore, it requires further study to investigate what factors suppress the gap in realistic conditions.

Many articles have tried to explain what led to the reduction in the activation gap. Earlier Hartree-Fock calculations show that the finite width and the Landau level mixing (LLM) can lower the skyrmion gaps [18–20]. A two-dimensional (2D) fixed-phase diffusion Monte Carlo (DMC) study by Melik-Alaverdian *et al.* [21] shows that while either the finite width or the LLM reduces the gap, the LLM has a much weaker influence for finite width systems. While all these studies show that the LLM and the finite width effect are responsible for the reduction of the activation gap, there is still a difference between the experimental gap and the theoretical gap including the correction of all these effects. A disorder-averaged Hartree-Fock calculation performed by Murthy shows that the effect of disorder may play a key role in reducing the excitation gap [29]. Another study by Wan *et al.* based on the calculation of Chern number [30] also shows the significance of disorder. These studies show that the activation gap is generally reduced in the presence of disorders, with or without the skyrmion physics. However, to the best of our knowledge, there is no work so far that includes the influence of the finite width, the LLM, and disorder altogether. Therefore, a model that quantitatively captures all these factors in a realistic manner is needed.

In this paper, we report on our three-dimensional (3D) fixed-phase DMC study of the skyrmion gap of a $\nu = 1$ system in the presence of charged impurities. Our study includes the LLM, the finite width effect, and the influence of charged impurities simultaneously. Our calculation shows that without any impurities, the LLM and the finite width effect are not sufficient to reduce the activation gap to the value that has been observed in experiments. On the other hand, within our model, charged impurities that interact with the system by Coulomb interaction lead to an additional reduction in the activation gap. The calculated gap in the presence of charged impurities agrees with experiments reasonably well, given that all the characteristic parameters of impurities are in the range

that is allowed by standard GaAs quantum well experiments [22,23]. We also find that the charged impurities suppress the size of skyrmions.

In the following sections, we first review the background of the skyrmion physics at $\nu = 1$. We next show our variational Monte Carlo (VMC) as well as DMC studies of the change of the gap due to the finite width and the LLM effect without any impurities. Finally, we show how the charged impurities influence the gap, and compare our results with experiments.

II. $\nu = 1$ SKYRMION

In this section, we briefly review the background of the skyrmion physics. Throughout this paper, we specify the unit of length to be the magnetic length $l_B = \sqrt{\frac{\hbar c}{eB}}$ and the unit of energy to be the Coulomb energy $e^2/\varepsilon l_B$. We also define the LLM parameter κ to be the ratio between the Coulomb energy and the cyclotron energy $\kappa = \frac{e^2/\varepsilon l_B}{\hbar\omega_c}$, where $\omega_c = \frac{eB}{mc}$. We work with the spherical geometry, where a magnetic monopole of the strength Q is placed at the center of the sphere to generate the uniform magnetic field on the surface, which produces a magnetic flux of $2Qhc/e$. Before we introduce the skyrmion wave functions, it is necessary to first give the ground state wave function for the quantum Hall state at $\nu = 1$ and the quasiparticle as well as the quasihole wave functions. The ground state wave function at $\nu = 1$ is obtained by filling up all the lowest Landau level orbitals. This requires the number of electrons N and the magnetic strength Q to satisfy $2Q + 1 = N$. The ground state wave function (unnormalized) reads

$$\Psi_{\mathrm{gs};N} = \prod_{1\leqslant j<k\leqslant N} (u_j v_k - u_k v_j), \tag{1}$$

where $u_i = \cos(\theta_i/2)e^{i\phi_i/2}$ and $v_i = \sin(\theta_i/2)e^{-i\phi_i/2}$ are spinor coordinates [31,32] of the ith particle, where θ_i and ϕ_i are the usual spherical angles. Because of the rotational symmetry, the quasiparticle and quasihole wave functions are most conveniently constructed by adding or removing electrons at the north or the south pole. In this paper, because we are calculating the energies of the quasihole and quasiparticle states independently and thus no interaction between the quasiparticle and quasihole is involved, it is in principle allowed to put the quasiparticle (hole) at either pole. Nonetheless, we place the quasihole at the north pole and the quasiparticle at the south pole for the convenience of description. We refer readers to Ref. [12] for a systematic study of Landau orbitals and quasiparticle (hole) wave functions on the sphere.

The quasihole wave function is obtained by removing an electron from the ground state at the north pole of the sphere by setting $u_N = 0$ and $v_N = 1$:

$$\Psi_{\mathrm{h};N-1} = \prod_{1\leqslant j<k<N} (u_j v_k - u_k v_j) \prod_{1\leqslant j<N} u_j. \tag{2}$$

We note that because for the ground state and the quasihole wave functions, only the spin-up orbitals are occupied, we do not write down the spins explicitly. We will write down the spin part of the wave functions explicitly when we give wave functions for the quasiparticle state and the skyrmion state to avoid any confusion since those two states involve both spins.

To calculate the excitation gap, we also need the wave function for the quasiparticle state. The wave function is constructed by adding an electron to the ground state at the south pole of the sphere:

$$\Psi_{\mathrm{p},N+1} = \mathcal{A}[\Psi_{1,N} Y_{QQ(-Q)}] \uparrow_1 \cdots \uparrow_N \downarrow_{N+1}], \tag{3}$$

where $\mathcal{A}$ is the antisymmetrization operator, $\uparrow$ and $\downarrow$ denote up and down spins, and $Y_{QQ(-Q)}$ is the magnetic harmonic in the LLL with the maximum quantum number for L_z[12]:

$$Y_{QQ(-Q)} = \left[\frac{2Q+1}{4\pi}\right]^{1/2} v^{2Q}. \tag{4}$$

We use the skyrmion wave function on the sphere proposed by MacDonald *et al.* [33]. The skyrmion wave function for $N-1$ particles with $K+1$ spins flipped relative to the ground state is given by

$$\Psi^K_{\mathrm{sk};N-1} = \Psi_{\mathrm{gs},N-1} \sum_{\{i_1,\ldots,i_K\}} [v_{i_1}\ldots v_{i_K} u_{j_1}\ldots u_{j_{N-1-K}} \times \downarrow_{i_1} \cdots \downarrow_{i_K} \uparrow_{j_1} \cdots \uparrow_{j_{N-1-K}}], \tag{5}$$

where the sum is over all distinct particle indices and j's denote the particles other than $i_1, i_2, \ldots, i_K$. When $K = 0$, the above wave function becomes the quasihole wave function, i.e., $\Psi_{\mathrm{h};N-1} = \Psi^{K=0}_{\mathrm{sk};N-1}$, as expected.

In principle, one can also obtain the wave function for the antiskyrmion by applying the particle-hole (PH) conjugation on the skyrmion wave function in the Fock space. However, we do not include this state in our study because of the reasons that we are going to discuss shortly.

The gap for flipping a single particle is defined as

$$\Delta_{\mathrm{ph}} = E_{\mathrm{p}} + E_{\mathrm{h}} - 2E_{\mathrm{gs}} + E_{\mathrm{Z}}. \tag{6}$$

Here E_{p} is the total energy of the quasiparticle state with $N+1$ particles, E_{h} is the total energy with $N-1$ particles, and E_{gs} is the ground state energy of N particles. The gap of the skyrmion-antiskyrmion pair of $S = 2K+1$ total spins flipped is defined as

$$\Delta_{\mathrm{sk\text{-}ask}}(K) = E_{\mathrm{sk}}(K) + E_{\mathrm{ask}}(K) - 2E_{\mathrm{gs}} + (2K+1)g, \tag{7}$$

where g is the Landé g factor and the relationship that $E_{\mathrm{Z}} = Sg$ has been used. When the LLM is not considered, the PH symmetry is preserved. In this case the energies of generating a pair of quasihole-skyrmion and a pair of quasiparticle-antiskyrmion are the same. Therefore one can rewrite Eq. (7) as

$$\Delta_{\mathrm{sk\text{-}ask}}(K) = \Delta_{\mathrm{ph}} + 2\delta(K), \tag{8}$$

where $\delta(K) = E_{\mathrm{sk}} - E_{\mathrm{h}} = E_{\mathrm{ask}} - E_{\mathrm{p}}$. On the other hand, when the PH symmetry is broken by the LLM, Eq. (8) does not hold anymore and one needs to explicitly calculate the gap of generating a pair of skyrmion and antiskyrmion to obtain the proper excitation gap. However, the antiskyrmion state is very difficult to handle in the DMC algorithm, which prevents us from performing an explicit calculation for antiskyrmion state. Nonetheless, we will continue to use Eq. (8) even when LLM is present. This is because the LLM typically only makes a small modification on the energy and only breaks the PH symmetry slightly at experimental parameters [34–37]. Compared to the big energy discrepancy that we are concerned

with throughout this paper, Eq. (8) is still a very accurate estimation of the activation gap.

For an infinite system, there is no upper limit of K. However, for a finite system of N particles, the maximum value of K is $N/2$. In general, $\Delta_{\text{sk-ask}}$ of different K values are different, and the actual K observed in the experiment is the one that gives the lowest energy. To determine the value of K, we use the Monte Carlo methods to calculate the energies of skyrmion states at all possible K's separately and pick out the one that has the lowest $\Delta_{\text{sk-ask}}$.

III. VARIATIONAL MONTE CARLO STUDY

In this section we introduce our VMC study of the problem. There are two different calculations that are performed. First, we neglect the finite width of the quantum well. Next, we perform a calculation that includes the finite width effect of the quantum well by taking the effective Coulomb interaction between particles as

$$V_{\text{eff}}(r) = \int dz_1 \int dz_2 \frac{\rho(z_1)\rho(z_2)}{\sqrt{r^2 + (z_1 - z_2)^2}}, \tag{9}$$

where $\rho(z)$ is the transverse distribution, which is evaluated in local density approximation at zero magnetic field [8,38]. In our study, the width of the quantum well is sufficiently narrow that only the lowest subband is involved. (We choose the parameters similar to those in Refs. [22,23] where the carrier densities are around 10^{11} cm^{-2} and the quantum well widths are around 20 nm, which corresponds to a width of $1 - 2l_B$.)

The results are shown in Fig. 1. We find that the finite width effect can reduce the energy gap by about 20%–30%. The gap after the inclusion of finite width is still significantly greater than experimental values. We note that our results agree with earlier Hartree-Fock and Monte Carlo calculations [18–20]. We also show the total number of reversed spins S from our calculation. The smallest system has 24 particles so the largest K considered in our calculation is 12. This sets an upper limit of S in our calculation to be 25.

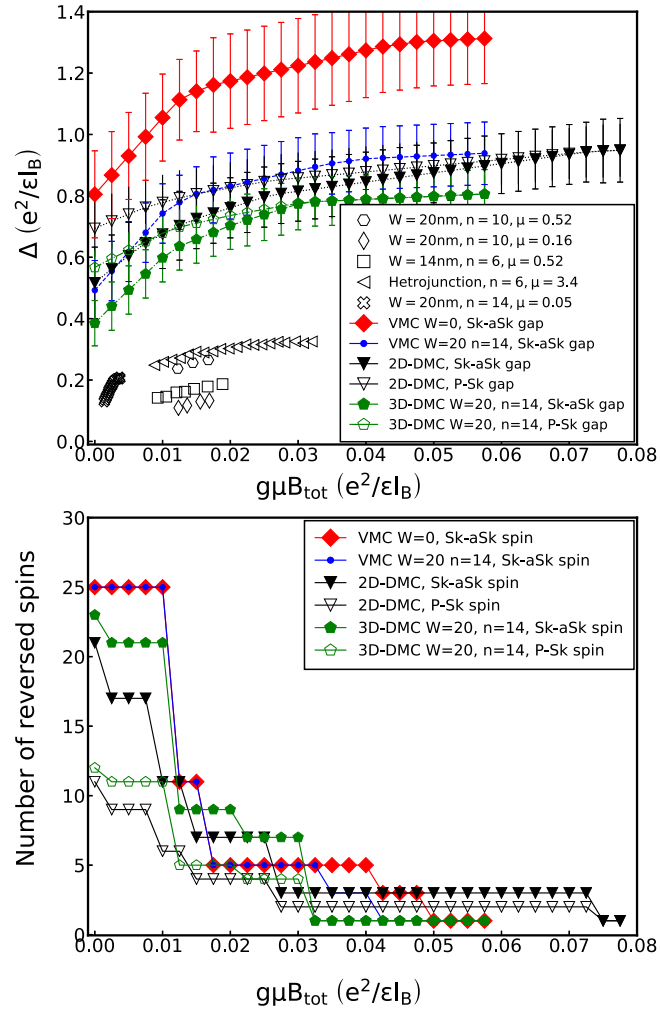

FIG. 1. The gap and the total number of reversed spins calculated by VMC and DMC methods for skyrmion states at $\nu = 1$. Top: experimental and theoretical gaps at different parameters. Bottom: the total number of reversed spins calculated by VMC and DMC methods. In the legend, W stands for the quantum well width in nanometers and n stands for the carrier density in 10^{10} cm^{-2}. Experimental data are plotted with scattered marks with the mobilities labeled by μ in units of 10^6 cm^2/V s.

IV. DIFFUSION MONTE CARLO STUDY

Because the VMC results suggest that the finite width itself is not sufficient to explain the reduction in the activation gap, we proceed to explore how LLM influences the gap. This is done by the fixed-phase DMC calculation. The fixed-phase DMC is a type of the DMC method and it is specialized to solve the many-body Schrödinger equation where the wave functions for the system cannot be written as real functions (e.g., FQHE systems where time-reversal symmetry is broken). Essentially, this method approximates the phase of the ground state wave function by the phase of a well-defined trial wave function Ψ_{T} and uses the standard DMC technique to solve for the amplitude of the wave functions. In this paper, we consider both 2D and 3D cases. For 2D DMC, the trial wave functions are chosen to be the ansatz wave functions introduced above (Ψ_{gs}, Ψ_h, Ψ_p, or Ψ_{sk}). The trial wave function for 3D DMC is chosen to be the product of the 2D wave function and the transverse wave function:

$$\Psi_{\text{T}} = \Psi \prod_i \psi(z_i), \tag{10}$$

where Ψ is one of Ψ_{gs}, Ψ_{h}, Ψ_{p}, or Ψ_{sk}, and $\prod_i \psi(z_i) = \prod_i \cos(\frac{\pi z_i}{W})$ is the transverse trial wave function in the infinite square well of the width W. We note that the real GaAs quantum well is not infinitely deep. However, the systematic bias due to the infinite well approximation is negligible, because the penetration of the transverse wave function into the wall is small in a typical situation [37].

Compared with the VMC, in which the wave function is always lowest Landau level projected, the DMC algorithm does not restrict the final state to be lowest Landau level projected and it allows the mixing with higher Landau levels. The LLM in the DMC is controlled by the LLM parameter κ. In the limit of $\kappa \to 0$, the DMC calculation degrades to the

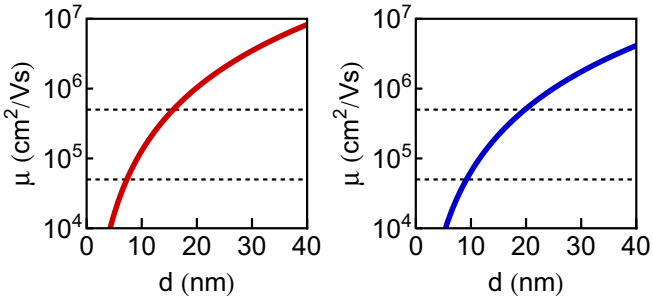

FIG. 2. The mobility due to Coulomb scattering as a function of the impurity separation d, calculated with the Born approximation. Left: $Z = 0.5$ and $n_{\rm imp} = 2.8 \times 10^{11}$ cm^{-2}. Right: $Z = 1$ and $n_{\rm imp} = 1.4 \times 10^{11}$ cm^{-2}. The dashed lines show the mobility values observed in Ref. [22] ($\mu = 5 \times 10^4$ cm^2/ V s, $n = 1.4 \times 10^{11}$ cm^2/ V s) and Ref. [23] ($\mu = 5 \times 10^5$ cm^2/V s, $n = 10^{11}$ cm^{-2}).

VMC [45,46]. For $\nu = 1$, $\kappa = 1.07$ at $n = 1.4 \times 10^{11}$ cm^{-2}. The DMC method has been proven to be effective in solving FQHE problems [21,34,36,39–44] and we also refer readers to Refs. [45,46] for general introduction of the standard DMC. Some technical details of the 3D DMC method can also be found in Ref. [37].

In Fig. 1 we also show our DMC results. First we show the 2D DMC result in which the system is strictly 2D. Next we show the 3D DMC result in which the finite width effect is automatically included. We find that LLM itself can reduce the gap by about 20%–30%, which is comparable to the reduction caused by finite width effect alone. When both LLM and finite width are considered, the gap is only further decreased by very little. The fact that the LLM has a much weaker effect for finite width systems agrees with the conclusion in Ref. [21]. This is not very surprising, as the finite width effect softens the repulsion between particles, less mixing with higher Landau levels is needed.

V. THE ROLE OF CHARGED IMPURITY

Based on our results from VMC and DMC, we find that the LLM and finite width are not sufficient to explain the discrepancy between theory and experiments. Another important factor that has not been included in our study is the

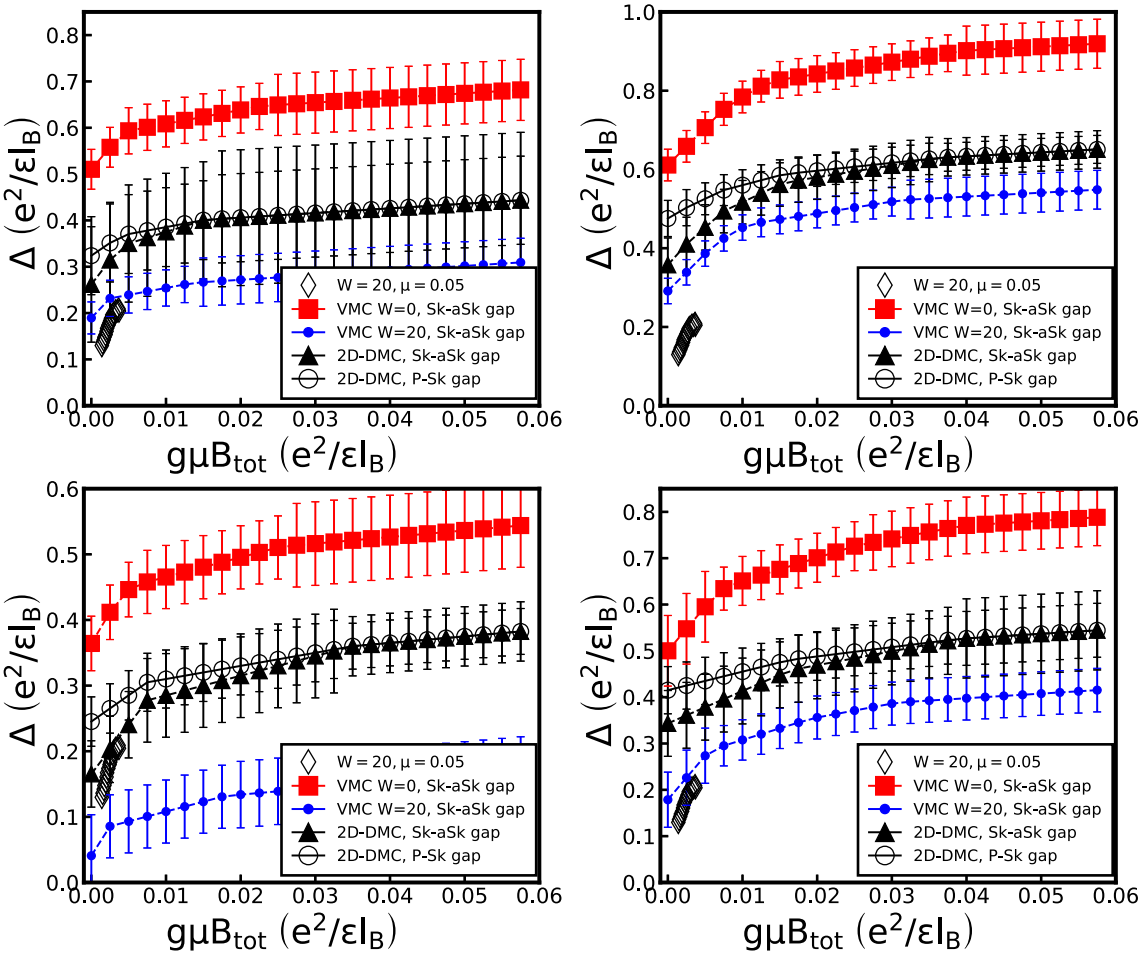

FIG. 3. The activation gap calculated by VMC and 2D DMC methods for skyrmion at $\nu = 1$ with charged impurity q separated from the quantum well by the distance d. Top left: $q = 0.5e$ and $d = 10$ nm. Top right: $q = 0.5e$ and $d = 20$ nm. Bottom left: $q = e$ and $d = 20$ nm. Bottom right: $q = e$ and $d = 30$ nm. In the legend, W stands for the quantum well width in nanometers and μ is the mobility in 10^6 cm^2/V s. The LLM of 2D DMC is $\kappa = 1$, which corresponds to $n = 1.4 \times 10^{11}$ cm^{-2}. Experimental data are drawn with scattered points for comparison.

influence of disorders. It is believed that at low temperatures, the scattering process is dominated by charged impurities via the Coulomb interaction [47]. This is partially justified by the fact that the theoretically calculated mobility due to the Coulomb scattering agrees with experiments [48–50]. For our purpose, we consider a simple model: a negatively charged impurity q is placed above the north pole of the sphere and a charged $-q$ impurity is placed above the south pole. We place the impurities at these locations because in general quasiholes are attracted to negative charges and quasiparticles are attracted to positive charges. Since we add the quasihole at the north pole and the quasiparticle at the south pole, such a configuration should be energetically favored. We also note that because only one skyrmion-antiskyrmion pair is inside our system, there is only one pair of charged impurities. This configuration is only suitable to study sparsely distributed impurities since each skyrmion is only affected by one impurity. We next specify the separation between the impurities and the quantum well to be some values of the order of a few hundred angstroms. The separation is chosen as such because experimentally the Coulomb impurities are typically introduced in a doping region that is separated from the quantum well by a few hundreds of angstroms. We will see shortly that this is also supported by a quantitative calculation of the mobility through estimating the relaxation time ($\mu = \frac{e\tau}{m}$) due to the Coulomb scattering. In general, one needs a sophisticated model to properly include the effects from finite width of the quantum well, the distribution of impurities, and the screening effect on the permittivity [47,51]. However, because we do not know all these details, we can only look for a semiquantitative description of the disorder at best. The mobility of the 2D electron gas in the Born approximation at zero temperature reads [51]

$$\mu = \frac{8e(k_F d)^3}{Z^2 \pi \hbar n_{\text{imp}}}, \tag{11}$$

where d is the separation between the impurity and the 2D system, k_F is the Fermi wave vector, Ze is the impurity charge, and n_{imp} is the 2D density of impurities. In our study, we make the assumption that the total charge of impurities is the same as the total charge of electrons, i.e., $Zn_{\text{imp}} = n$. In Fig. 2, we show that for $Z = 0.5$ and $Z = 1$, this model gives a mobility that agrees with the value measured in experiments [22,23] when d is around 10–30 nm.

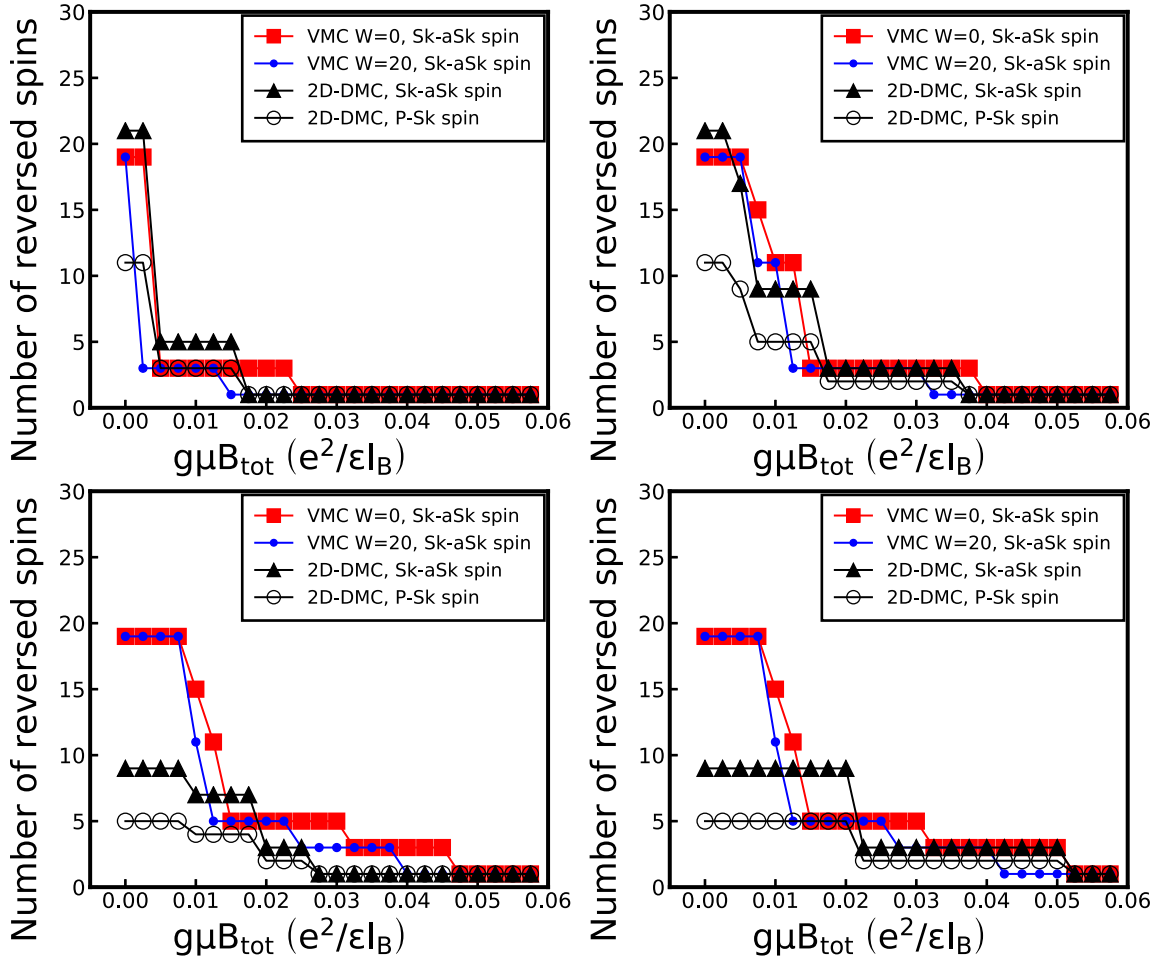

FIG. 4. The number of total reversed spins of skyrmions at different impurity separations d calculated by VMC and 2D DMC in the presence of charged impurities in the quantum well at $n = 1.4 \times 10^{11}$ cm^{-2}. Top left: $d = 10$ nm. Top right: $d = 20$ nm. Bottom left: $d = 30$ nm. Bottom right: $d = 40$ nm.

The results from VMC and 2D DMC calculation are shown in Fig. 3. In general, we find that the inclusion of charged impurities leads to a much better agreement between the theoretical and the experimental values of the activation gap. We find that for both impurity charges ($q = e$ and $q = 0.5e$), the skyrmion physics arises at small Zeeman energy and the gaps are comparable to experiments. Our calculation also gives the values of S at different g's. Our calculation suggests that the skyrmion physics can survive a wide range of charged impurity strength and distance. Particularly, a system with a large impurity charge and a large impurity distance can coincide with a system with a small impurity charge and a small impurity distance in their gaps. This gives a possible explanation for why the samples from Ref. [23] and Ref. [22] have very similar excitation gaps while their mobilities differ by about ten times. Lastly we show that there is a suppression effect on the skyrmion size due to the presence of impurities. As one can see in Fig. 4, when we fix the impurity charge to be $0.5e$, the occurrence of the large size skyrmions ($S > 2$) is delayed as the charge distance decreases. This can be understood by the fact that the skrymion with a large K value has its charge distribution more extended, so the pointlike impurity has a stronger attraction with small skyrmions. The calculation suggests that in order to obtain large-size skyrmions experimentally, the charged impurities should be separated from the quantum well distantly.

VI. CONCLUSION

In this paper, we have revisited the question of the discrepancy between the theoretically calculated and experimentally measured activation gaps in the $\nu = 1$ quantum Hall state. We have found that the puzzle cannot be resolved by only considering the finite width effect and the LLM effect. We have proposed a simple model to include the influence of sparsely distributed charged impurities and our conclusion is that the Coulomb impurities can greatly reduce the activation gap and they can also suppress the size of skyrmions. While our model can explain the experimental observations, it may lack realistic details, and thus our model is at its best a semiquantitative account of the puzzle. More experiments are required to further elucidate this issue.

ACKNOWLEDGMENTS

I am grateful to J. K. Jain for our discussion on the results and his advice on the paper. I would also like to thank Mansour Shayegan and Ganpathy Murthy for many insightful discussions. The work was made possible by financial support from the U.S. Department of Energy under Award No. DE-SC0005042. The numerical calculations were performed using Advanced CyberInfrastructure computational resources provided by The Institute for CyberScience at The Pennsylvania State University.

[1] H. L. Stormer, D. C. Tsui, and A. C. Gossard, Rev. Mod. Phys. **71**, S298 (1999).
[2] D. C. Tsui, H. L. Stormer, and A. C. Gossard, Phys. Rev. Lett. **48**, 1559 (1982).
[3] R. B. Laughlin, Phys. Rev. B **23**, 5632 (1981).
[4] J. K. Jain, Phys. Rev. Lett. **63**, 199 (1989).
[5] G. S. Boebinger, A. M. Chang, H. L. Stormer, and D. C. Tsui, Phys. Rev. Lett. **55**, 1606 (1985).
[6] R. L. Willett, H. L. Stormer, D. C. Tsui, A. C. Gossard, and J. H. English, Phys. Rev. B **37**, 8476 (1988).
[7] R. R. Du, H. L. Stormer, D. C. Tsui, L. N. Pfeiffer, and K. W. West, Phys. Rev. Lett. **70**, 2944 (1993).
[8] K. Park, N. Meskini, and J. Jain, J. Phys.: Condens. Matter **11**, 7283 (1999).
[9] V. W. Scarola, S.-Y. Lee, and J. K. Jain, Phys. Rev. B **66**, 155320 (2002).
[10] W. Pan, W. Kang, M. P. Lilly, J. L. Reno, K. W. Baldwin, K. W. West, L. N. Pfeiffer, and D. C. Tsui, Phys. Rev. Lett. **124**, 156801 (2020).
[11] K. A. V. Rosales, P. T. Madathil, Y. J. Chung, L. N. Pfeiffer, K. W. West, K. W. Baldwin, and M. Shayegan, Phys. Rev. Lett. **127**, 056801 (2021).
[12] J. K. Jain, *Composite Fermions* (Cambridge University Press, Cambridge, 2007).
[13] R. Morf and B. I. Halperin, Phys. Rev. B **33**, 2221 (1986).
[14] F. D. M. Haldane and E. H. Rezayi, Phys. Rev. Lett. **54**, 237 (1985).
[15] S. M. Girvin, A. H. MacDonald, and P. M. Platzman, Phys. Rev. Lett. **54**, 581 (1985).
[16] M. W. Ortalano, S. He, and S. Das Sarma, Phys. Rev. B **55**, 7702 (1997).
[17] K. Park and J. K. Jain, Phys. Rev. Lett. **83**, 5543 (1999).
[18] H. A. Fertig, L. Brey, R. Côté, A. H. MacDonald, A. Karlhede, and S. L. Sondhi, Phys. Rev. B **55**, 10671 (1997).
[19] N. R. Cooper, Phys. Rev. B **55**, R1934 (1997).
[20] I. Mihalek and H. A. Fertig, Phys. Rev. B **62**, 13573 (2000).
[21] V. Melik-Alaverdian, N. E. Bonesteel, and G. Ortiz, Phys. Rev. B **60**, R8501 (1999).
[22] S. P. Shukla, M. Shayegan, S. R. Parihar, S. A. Lyon, N. R. Cooper, and A. A. Kiselev, Phys. Rev. B **61**, 4469 (2000).
[23] A. Schmeller, J. P. Eisenstein, L. N. Pfeiffer, and K. W. West, Phys. Rev. Lett. **75**, 4290 (1995).
[24] E. H. Rezayi, Phys. Rev. B **36**, 5454 (1987).
[25] E. H. Rezayi, Phys. Rev. B **43**, 5944 (1991).
[26] S. L. Sondhi, A. Karlhede, S. A. Kivelson, and E. H. Rezayi, Phys. Rev. B **47**, 16419 (1993).
[27] X. C. Xie and S. He, Phys. Rev. B **53**, 1046 (1996).
[28] A. Wójs and J. J. Quinn, Phys. Rev. B **66**, 045323 (2002).
[29] G. Murthy, Phys. Rev. B **64**, 241309(R) (2001).
[30] X. Wan, D. N. Sheng, E. H. Rezayi, K. Yang, R. N. Bhatt, and F. D. M. Haldane, Phys. Rev. B **72**, 075325 (2005).
[31] F. D. M. Haldane, Phys. Rev. Lett. **51**, 605 (1983).
[32] T. T. Wu and C. N. Yang, Nucl. Phys. B **107**, 365 (1976).
[33] A. H. MacDonald, H. A. Fertig, and L. Brey, Phys. Rev. Lett. **76**, 2153 (1996).
[34] V. Melik-Alaverdian, N. E. Bonesteel, and G. Ortiz, Phys. Rev. Lett. **79**, 5286 (1997).

[35] G. J. Sreejith, Y. Zhang, and J. K. Jain, Phys. Rev. B **96**, 125149 (2017).
[36] J. Zhao, Y. Zhang, and J. K. Jain, Phys. Rev. Lett. **121**, 116802 (2018).
[37] T. Zhao, W. N. Faugno, S. Pu, A. C. Balram, and J. K. Jain, Phys. Rev. B **103**, 155306 (2021).
[38] M. Rother, 2D Schroedinger Poisson solver AQILA, https://www.mathworks.com/matlabcentral/fileexchange/3344-2d-schroedinger-poisson-solver-aquila.
[39] A. D. Güçlü, G. S. Jeon, C. J. Umrigar, and J. K. Jain, Phys. Rev. B **72**, 205327 (2005).
[40] G. Ortiz, D. M. Ceperley, and R. M. Martin, Phys. Rev. Lett. **71**, 2777 (1993).
[41] V. Melik-Alaverdian and N. E. Bonesteel, Phys. Rev. B **52**, R17032 (1995).
[42] F. Bolton, Phys. Rev. B **54**, 4780 (1996).
[43] Y. Zhang, A. Wójs, and J. K. Jain, Phys. Rev. Lett. **117**, 116803 (2016).
[44] M. S. Hossain, M. A. Mueed, M. K. Ma, K. A. Villegas Rosales, Y. J. Chung, L. N. Pfeiffer, K. W. West, K. W. Baldwin, and M. Shayegan, Phys. Rev. Lett. **125**, 046601 (2020).
[45] P. J. Reynolds, D. M. Ceperley, B. J. Alder, and W. A. Lester, Jr., J. Chem. Phys. **77**, 5593 (1982).
[46] W. M. C. Foulkes, L. Mitas, R. J. Needs, and G. Rajagopal, Rev. Mod. Phys. **73**, 33 (2001).
[47] T. Ando, A. B. Fowler, and F. Stern, Rev. Mod. Phys. **54**, 437 (1982).
[48] T. Ando, J. Phys. Soc. Jpn. **51**, 3900 (1982).
[49] J. P. Harrang, R. J. Higgins, R. K. Goodall, P. R. Jay, M. Laviron, and P. Delescluse, Phys. Rev. B **32**, 8126 (1985).
[50] L. Zheng and S. Das Sarma, Phys. Rev. B **53**, 9964 (1996).
[51] J. H. Davies, *The Physics of Low-Dimensional Semiconductors: An Introduction* (Cambridge University Press, Cambridge, UK, 1998).